Chinese Chemical Letters 37 (2026) 111292

Contents lists available at ScienceDirect

Chinese Chemical Letters

journal homepage: www.elsevier.com/locate/cclet

Colon-targeted pellets encapsulating patchouli oil cocrystal for inflammatory bowel disease treatment

Zeyu Li[a,b], Huan Shen[b], Wenli Cai[a,b], Quangang Xu[b,d], Wei Xia[b,e], Keke Ning[b,f], Ergang Liu[b,*], Yongzhuo Huang[a,b,c,*]

[a] Key Laboratory of Chronic Disease Prevention and Control of Traditional Chinese Medicine of Guangdong Higher Education Institutes, School of Chinese Materia Medica, Guangzhou University of Chinese Medicine, KLGHEI (2024KSYS024), Guangzhou 510006, China
[b] Zhongshan Institute for Drug Discovery, Shanghai Institute of Materia Medica, Chinese Academy of Sciences, Zhongshan 528400, China
[c] Shanghai Institute of Materia Medica, Chinese Academy of Sciences, Shanghai 201203, China
[d] School of Pharmacy, Guizhou Medical University, Guizhou 561113, China
[e] School of Traditional Chinese Pharmacy, Nanjing University of Chinese Medicine, Nanjing 210023, China
[f] Zunyi Medical University, Zunyi 563006, China

ARTICLE INFO

Article history:
Received 12 January 2025
Revised 28 April 2025
Accepted 8 May 2025
Available online 10 May 2025

Keywords:
Patchouli oil
Cyclodextrin
Inclusion cocrystal
Inflammatory bowel disease
Colon-targeted delivery

ABSTRACT

Patchouli oil (PAO), a traditional herbal remedy with notable anti-inflammatory properties, has demonstrated significant therapeutic potential in gastrointestinal diseases. However, its instability in acidic environments and low bioavailability hinder PAO's clinical application. In this study, we developed a pharmaceutical solid-state form of PAO using a β-cyclodextrin (βCD)-based inclusion cocrystal technology, thus obtaining PAO-βCD cocrystals. PAO-βCD cocrystals exhibited enhanced dissolution and stability. We further encapsulated them in pH-sensitive Eudragit-coated pellets (PAO-βCD@pellet) to achieve site-specific delivery of PAO to the inflamed colon. *In vivo* results from the dextran sulfate sodium salt (DSS)-induced colitis mouse model showed that PAO-βCD@pellet significantly improved the colonic release of PAO, as evidenced by fluorescence tracking and quantitative analysis of patchouli alcohol, the main active compound of PAO. Furthermore, PAO-βCD@pellet demonstrated superior therapeutic efficacy, reducing disease activity index, preventing intestinal barrier damage, and modulating the gut microbiome. Histological examination confirmed alleviating intestinal epithelial cell damage caused by oxidative stress and inflammation. These findings suggest that PAO-βCD@pellet offers a promising targeted treatment strategy for inflammatory bowel disease (IBD) with enhanced stability, bioavailability, and therapeutic outcomes.

© 2026 Published by Elsevier B.V. on behalf of Chinese Chemical Society and Institute of Materia Medica, Chinese Academy of Medical Sciences.

Inflammatory bowel disease (IBD) is a chronic, relapsing disorder of the bowel with an unclear etiology. Patients with IBD suffer greatly from recurrent fever, weight loss, rectal bleeding, diarrhea, and abdominal pain [1], significantly affecting life quality. Available treatments primarily focus on symptom alleviation using 5-aminosalicylic acid (5-ASA), corticosteroids, immunomodulators, and biologics [2–4], but providing short-term relief [5]. Their prolonged use against recurrent inflammation may lead to resistance and significant adverse effects [6]. Small-molecule drugs, such as Janus kinase (JAK) inhibitors, have shown promise, but their long-term efficacy and safety remain to be monitored [7–9]. Although biologics have become the first-line treatment for moderate to severe IBD, approximately 30% of patients exhibit primary non-response, and up to 50% may develop anti-drug antibodies, leading to secondary loss of response over time [10–12]. Thus, there is a pressing need for safe and effective options for long-term treatment of IBD.

Traditional Chinese medicine (TCM) provides a promising approach to treating gastrointestinal diseases with a long application history. Among these, *Guang-Huo-Xiang*, a patchouli herb (the aerial fractions of *Pogostemon cablin* (*Blanco*) Benth) has been widely used for its capability of alleviating symptoms of gastrointestinal diseases [13]. Patchouli oil (PAO) is the main active compounds from this herb, encompassing volatile compounds such as patchouli alcohol (PA), pogostone (PO), and patchoulene (PE), which possess anti-inflammatory, immune-modulatory, and potency for restoring colonic barrier and intestinal water absorption, thus manifesting therapeutic promise in IBD [14–16]. Nevertheless, PAO is a water-immiscible oil with low physical (volatile) and chemical (degrade under acidic conditions) stability, thereby complicating its pharmaceutical preparation and *in vivo* delivery [17].

* Corresponding authors.
E-mail addresses: liuergang@zidd.ac.cn (E. Liu), yzhuang@simm.ac.cn (Y. Huang).

https://doi.org/10.1016/j.cclet.2025.111292
1001-8417/© 2026 Published by Elsevier B.V. on behalf of Chinese Chemical Society and Institute of Materia Medica, Chinese Academy of Medical Sciences.

Given that the colon is the target site for IBD treatment, an ideal delivery system should guarantee a sufficient dose of the therapeutics without being metabolized in the stomach and small intestine [18]. It potentially provides an effective strategy for PAO-based IBD treatment.

Inclusion cocrystals are a class of cocrystals characterized by the host-guest interaction between cyclodextrins and drug molecules. Unlike conventional cyclodextrin-based inclusion complexes which are generally amorphous products with excess cyclodextrin, inclusion cocrystals are constituted by stoichiometrically coordinated drug molecules and cyclodextrins that form orderly crystalline structures [19]. These structures confer different physical properties (*e.g.*, melting point, powder density, and flowability) [19]. Moreover, the inclusion cocrystals can release drugs in the form of the inclusion complex, improving solubility, stability, and mitigating the harsh conditions of the gastrointestinal tract [19]. Herein, we proposed a novel strategy for enhancing the druggability of volatile oils by developing inclusion cocrystals of volatile oils and reported a formulation of PAO-β-cyclodextrin (βCD) inclusion cocrystals (PAO-βCD). Furthermore, to achieve colon-specific delivery, we designed a pH-sensitive Eudragit layer-coating pellet system for encapsulating PAO-βCD. It was expected that the pellets would be able to release PAO in the colon, with increased drug concentration and enhanced therapeutic efficacy of PAO on IBD.

We prepared PAO-βCD inclusion cocrystals *via* an anti-solvent method (Fig. 1A), through which the liquid PAO was transformed into crystalline solids (Fig. S1 in Supporting information). The formulation and preparation process were optimized by single-factor screening and orthogonal screening, respectively. The preparation conditions were optimized as follows: stirring speed of 200 rpm, stirring time of 1 min, temperature of 45 °C, and a ratio of PAO to cyclodextrin at 1:9 (Tables S1–S3 in Supporting information). The crystallization efficiency (CE, also known as production yield) of PAO-βCD was calculated to be 85.3 %. Scanning electron microscopy (SEM) of the products showed a cubic morphology (Fig. 1B) that different from βCD (Fig. S2 in Supporting information). The hydrodynamic size of PAO-βCD was around 2.7 μm (Fig. S3 in Supporting information). Fourier transform infrared spectroscopy (FTIR) showed that the characteristic peaks of PAO almost disappeared in PAO-βCD (Fig. 1C), suggesting that the functional groups of PAO components were encapsulated by hydrophobic cavities of βCD. Meanwhile, the FTIR spectrum of the inclusion cocrystal was similar to βCD with minor shifts in C–OH signals at 990 and 1022 cm^{-1}, respectively [20], indicating intermolecular interactions (*e.g.*, hydrogen binding and Vanderwal's force) within crystalline lattice (Fig. 1C) [19]. Powder X-ray diffraction (PXRD) further confirmed the crystal structure of the formed cocrystals, with diffraction peaks (5.7°, 6.4°, 6.6°, 6.7°, 10.9°, 11.6°, 14.2°, 14.5°, 15.1°, 15.5°, 16.8°, 17.1°, 17.3°, 17.9°, 18.3°, 20.7°, 24.0°, 24.5°) distinct from βCD or inclusion complexes of PAO and βCD (Fig. 1D). Differential scanning calorimetry (DSC) results showed that the melting point of PAO-βCD (about 319 °C) was higher than βCD (307 °C) (Fig. 1E). Thermogravimetric analysis (TGA) results showed a water loss from PAO-βCD was 8.6 %, significantly lower than βCD (12.5 %) (Fig. 1F). This indicated encapsulated PAO repelled the pre-existed water molecules in the cavities of cyclodextrins, in line with the FTIR results presuming PAO and βCD within the crystals were in the form of inclusion complex, which was favorable for improving solubility and stability.

We compared the PAO-βCD cocrystals with silica-adsorbed PAO (PAO-HMSN) and PAO-cyclodextrin inclusion complexes (PAO/βCD) (two common pharmaceutical strategies for solidifying volatile oils). Storage stability experiments showed that free PAO was markedly degraded at 60 °C, with only 22.0 % remaining after 3-day storage (Fig. 1G), while PAO-HMSN and PAO/βCD retained 73.7 % and 81.3 % of PAO, respectively. Notably, PAO-βCD exhibited the highest stability, maintaining 94.7 % of PAO after 3-day storage. Extending the accelerated storage to 1 week still detected 82.7 % of PAO in the PAO-βCD, whereas PAO-HMSN and PAO/βCD retained only 55.3 % and 29.0 % of PAO, respectively. This suggested that the formation of cocrystals conferred superior thermostability. In addition, given that the PAO components primarily resided in the cyclodextrin cavity, PAO-βCD significantly improved the water solubility of PAO. The determined solubility of PAO-βCD was 100.8 μg/mL, 11 times higher than free PAO (<10 μg/mL) (Table S4 in Supporting information). As a result, the *in vitro* dissolution rate of PAO from PAO-βCD was faster compared to PAO-HMSN (Fig. 1H).

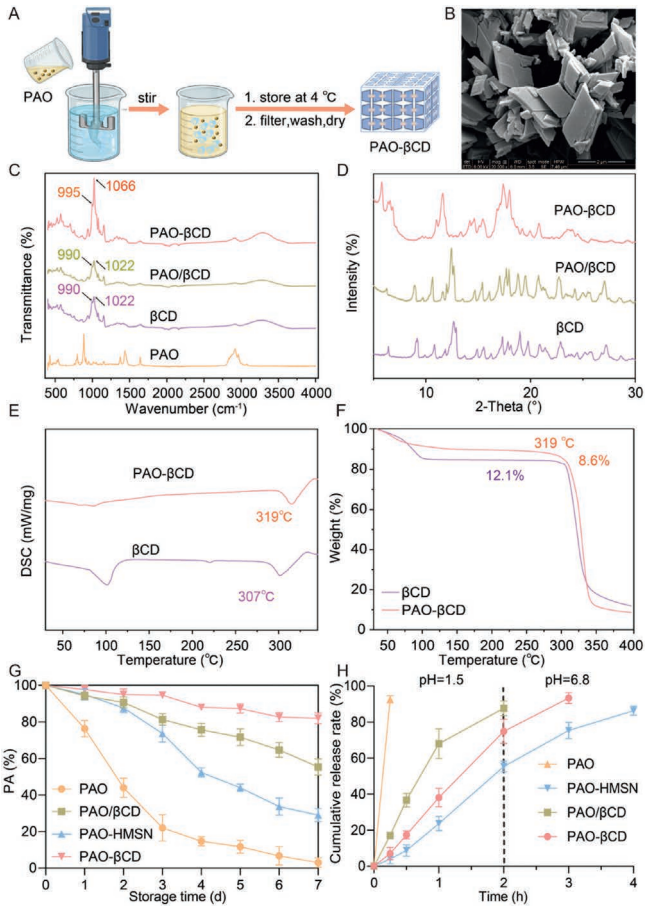


Fig. 1. Preparation and characterization of PAO-βCD cocrystals. (A) Schematic illustration of the preparation of PAO-βCD. (B) The SEM image of PAO-βCD cocrystals. Scale bar: 2 μm. (C) FTIR spectrum of free PAO, βCD, PAO/βCD, and PAO-βCD cocrystals. (D) PXRD patterns of βCD, PAO/βCD, and PAO-βCD cocrystals. (E) DSC profiles of βCD and PAO-βCD cocrystals. (F) TGA profiles of βCD and PAO-βCD cocrystals. (G) Storage stability of free PAO, PAO-HMSN, PAO/βCD, and PAO-βCD cocrystals at 60 °C. (H) *In vitro* release profiles of free PAO, PAO-HMSN, PAO/βCD, and PAO-βCD cocrystals. Data are presented as mean ± standard deviation (SD) ($n = 3$).

IBD primarily affects the colon and rectum, and it is critical to regulate the drug release to enhance drug exposure at the site of inflammation [2]. Given the rapid-release nature of the PAO-βCD cocrystals, direct oral administration could hardly reach effective drug concentrations in the colon. To address this, we prepared the PAO-βCD@pellet using an extrusion-spheronization method combined with coating technology. The pellets preparation process consisted of two steps: pellets were firstly prepared by extrusion and spheronization, followed by coating in a fluidized bed (Fig. 2A). The optimal formulation for pelletization was obtained through a single-factor analysis and orthogonal screening, with a composition of 44.5 % PAO-βCD, 22.2 % microcrystalline cellulose

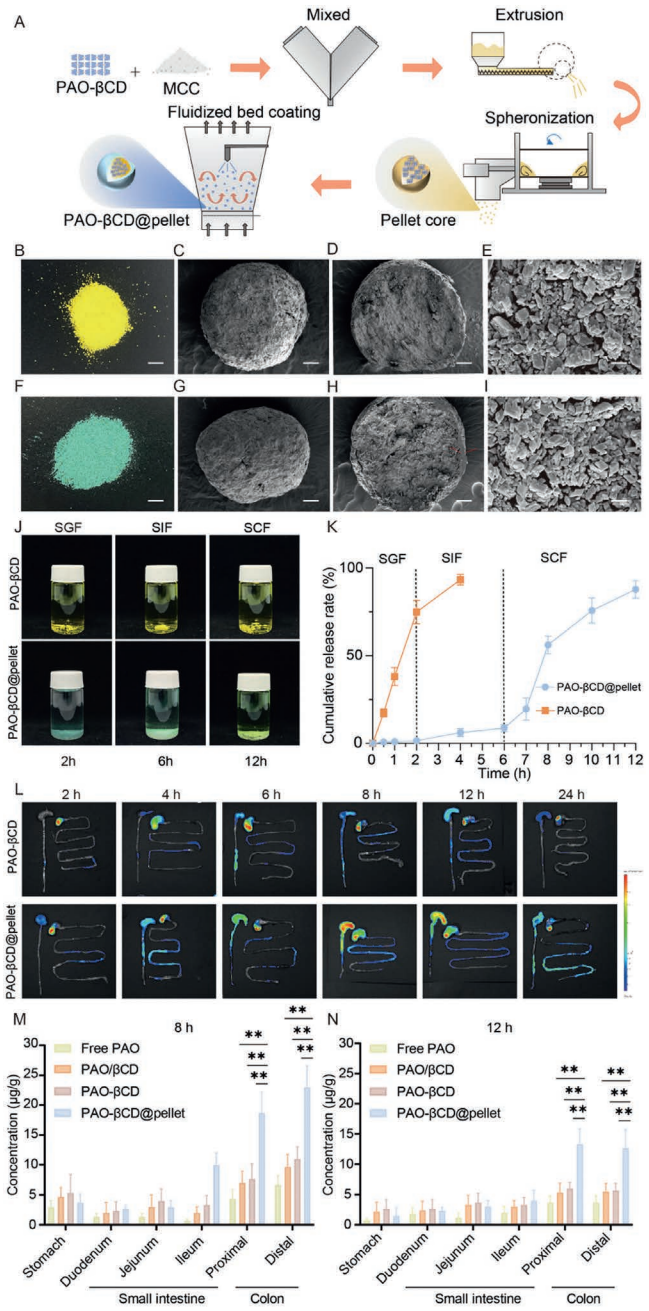


Fig. 2. Preparation, characterization, gastrointestinal distribution of PAO-βCD@pellet. (A) Scheme of preparing PAO-βCD@pellet. (B) PAO-βCD cocrystal pellet cores dyed by sunset yellow (scale bar: 5 cm). (C–E) SEM image (100-μm scale, C), and cross-section SEMs at 100-μm (D) and 2-μm scale (E), respectively, of a single PAO-βCD cocrystal pellet core. (F) PAO-βCD@pellets dyed by brilliant blue (scale bar: 5 cm). (G–I) SEM images (100-μm scale, G), and cross-section SEMs at 100-μm (H) and 2-μm scale (I), respectively, of a single PAO-βCD@pellet. (J) Stability of PAO-βCD and PAO-βCD@pellet in SGF/SIF/SCF. (K) *In vitro* release profiles of PAO-βCD@pellet and PAO-βCD cocrystals. (L) Fluorescence images of gastrointestinal tissues from the animals treated with PAO-βCD@pellet or PAO-βCD. Gastrointestinal quantitative distribution of PA at 8 h (M), and 12 h (N), from free PAO, PAO/βCD, PAO-βCD, and PAO-βCD@pellet by GC-FID. $^{**}P < 0.01$. Data are presented as mean ± SD) ($n = 3$).

(MCC), and 33.3 % water (as a wetting agent). PAO-βCD and MCC were firstly mixed, wetted by a predetermined amount of water, and subsequently placed in a spiral extruder equipped with a 0.9-mm sieve. The pellet cores were collected after rounding and drying (Fig. 2B and Tables S5–S7 in Supporting information). They displayed a bulk density of 0.79 g/mL with a yield of 81 % (Table S8 in Supporting information). For the coating step, the PAO-βCD pellet cores were coated with a mixed Eudragit layer (L100/S100, 1:4 wt ratio) *via* a fluidized-bed coating process. The overall weight increase after Eudragit coating was determined to be 3.0 %. SEM images of PAO-βCD displayed spherical morphology with a rough surface (Figs. 2B–E), which became smooth after coating (Figs. 2F–I). The Eudragit layer was observed with a thickness of about 30 μm (Fig. 2H).

The PAO-βCD@pellet was stable in a simulated gastric fluid (SGF, pH 1.2), but swelling in a simulated intestinal fluid (SIF, pH 6.8). Rapid dissolution occurred when the PAO-βCD@pellet were put in simulated colonic fluid (SCF, pH 7.4), where the pellets quickly swelled and eroded (Fig. 2J). *In vitro* release test (Fig. 2K) manifested the PAO-βCD@pellet released PAO most notably in SCF, suggesting the feasibility of site-specific release of encapsulated PAO in the colon. In contrast, PAO-βCD cocrystals rapidly dissolved and released PAO in the SGF. Considering the instability of PAO in acidic conditions [15], the fast dissolution of PAO-βCD was unfavorable for maintaining drug concentrations in the colon, which was essential for effective IBD treatment.

Colon-specific release potential of PAO-βCD@pellet was assessed by *in vivo* fluorescence imaging and quantitative gastrointestinal distribution of PAO after oral administration. Infrared-780 iodide (a lipophilic dye with maximum excitation wavelength at 780 nm) was dissolved in PAO for tracing the release behavior in the gastrointestinal tract [21]. All experimental protocols involving animals were meticulously conducted in compliance with institutional ethical standards and were approved by the Institutional Animal Care and Use Committee (IACUC) at the Zhongshan Institute for Drug Discovery. In line with the pH-dependent release *in vitro*, PAO-βCD cocrystals displayed fast dissolution, release, and excretion as evidenced by fast diminishing fluorescence in the mice (Figs. S4 and S5 in Supporting information). In comparison, the fluorescence of PAO-βCD@pellets remained stable for over 12 h. *Ex vivo* imaging of the excised gastrointestinal tracts demonstrated markedly enhanced colonic fluorescence in the group of PAO-βCD@pellets than the PAO-βCD group (Fig. 2L), indicating improved colon delivery of PAO. We further determined the time-dependent distribution of PAO in different regions of gastrointestinal tracts in rats by gas chromatography with a flame ionization detector (GC-FID). Quantitative results of PAO showed different distribution patterns of PAO-βCD@pellets compared to other groups. Due to the fast dissolution, PAO-βCD cocrystals rapidly released the encapsulated PAO after oral intake, similar to the distribution of PAO/βCD inclusion complex and free PAO. Consequently, PAO was mainly detected in the stomach and intestines in these three groups, with much less PAO detected in the colon at 4–6 h after administration (Fig. S6 in Supporting information). The colon PAO of PAO-βCD@pellet could still be observed at 24 h post-administration (Fig. 2L). In comparison, the PAO-βCD@pellet displayed a trace amount of PAO in gastro-intestines in the 4–6 h but accumulated in the colon at 8–12 h with a determined PAO of 18.7 μg/g, which is more than twice of the drug concentration of the other groups (Figs. 2M and N). This confirmed the colon-targeted delivery potency of PAO-βCD@pellet.

The therapeutic efficacy of PAO-βCD@pellet was evaluated in a DSS-induced acute colitis mouse model (Fig. 3A). Six groups of mice were included: control, model, sulfasalazine (Azulfidine), free PAO, PAO-βCD cocrystals, and PAO-βCD@pellet; all powder samples were dispersed in 80 % polyethylene glycol (PEG-400). Daily intake of 3 % DSS caused symptoms of intestinal inflammation, including mild-to-severe diarrhea, fecal occult blood, and body weight loss, contributing to increased disease activity index (DAI). DAI of the model group began to increase sharply on day 3 (Figs. 3B and C), indicating the onset of acute colitis. Treatment of free PAO resulted in a notable reduction in DAI and body weight

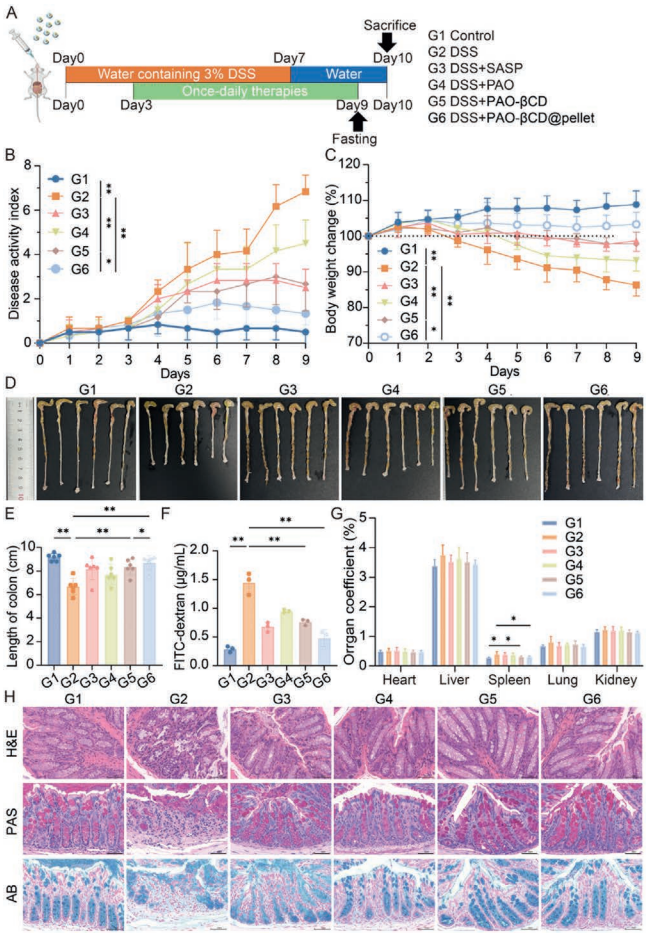


Fig. 3. *In vivo* treatment of IBD. (A) Schematic diagram of induction and treatment of colitis. (B) DAI and (C) body weight change during the treatment period. (D) Images and (E) length of the colons of mice. (F) The serum level of the FITC-dextran. (G) Organ coefficient of main organs. (H) Histopathological assessment of distal colon tissue sections stained with hematoxylin-eosin staining (H&E), periodic acid-Schiff staining (PAS), and alcian blue staining (AB). Scale bar: 50 μm. Data are presented as means ± SD ($n = 6$). $^{*}P < 0.05$, $^{**}P < 0.01$.

loss, supporting its potency as an active ingredient from patchouli for IBD treatment.

Crystallizing PAO into inclusion cocrystals improved its therapeutic effect, with DAI reduction comparable to the first-line drug SASP on day 9 (2.6 ± 1.1 *vs.* 2.5 ± 0.8). Given the *in vivo* dissolution and release profile of PAO-βCD cocrystals, the enhanced efficacy likely resulted from increased gastric stability of the released inclusion complex [22]. PAO-βCD@pellet further improved therapeutic outcomes, showing the least DAI (1.3 ± 0.5) and weight loss among all treatment groups. PAO-βCD@pellet also demonstrated a significant reduction in colon shortening (Figs. 3D and E) and prevented intestinal absorption of fluorescein isothiocyanate (FITC)-labeled dextran, with serum FITC-dextran levels comparable to the control group, suggesting that PAO-βCD@pellet effectively prevented DSS-induced damage to the intestinal barrier, maintaining intestinal permeability (Fig. 3F). Histological results revealed that PAO-βCD@pellet reduced colonic epithelial cell necrosis, crypt damage, and goblet cell loss (Fig. 3H), as compared with other groups.

A preliminary biosafety assessment was conducted by analyzing organ coefficients of the heart, liver, spleen, lung, and kidneys. The model group exhibited elevated spleen coefficient, indicative of systemic inflammation (Figs. 3F and G). Further histological analysis of organs (heart, liver, spleen, lung, and kidneys) in normal mice treated with 30 mg/kg of PAO, PAO-βCD, or PAO-βCD@pellet for 7 days showed no significant organ damage, confirming the safety of both PAO and its formulations (Fig. S7 in Supporting information). Reactive oxygen species (ROS) play a significant role in the development and progression of IBD [23], as well as in the onset and progression of DSS-induced colitis [24]. ROS can induce epithelial damage through pyroptosis [15] and activate immune responses, producing inflammatory cytokines and worsening intestinal damage [25]. We assessed ROS levels by measuring superoxide dismutase (SOD) activity, myeloperoxidase (MPO) activity, and malondialdehyde (MDA) levels, which were closely related to ROS production [26] and damage [27]. The model group exhibited a notable decline in SOD activity, accompanied by increased MPO activity and MDA levels. In contrast, PAO-βCD@pellet significantly elevated SOD activity while reducing MPO activity and MDA levels, indicating alleviation of oxidative stress in the colon (Figs. S8B–D in Supporting information). Subsequent analysis utilizing real-time quantitative polymerase chain reaction (RT-qPCR) demonstrated that PAO-βCD@pellet significantly diminished the expression of key inflammatory cytokines, specifically tumor necrosis factor-α (TNF-α), interleukin (IL)-1β, and IL-6 within the colonic tissue (Figs. S8E–G in Supporting information). Furthermore, these pellets effectively restored the expression of tight junction-associated proteins, including zonula occludens protein 1 (ZO-1), mucoprotein-2 (MUC-2), and claudin-4, supporting its potency in restoring the intestinal barrier from inflammatory damage. Overall, the most substantial effects were observed in the group of PAO-βCD@pellet (Figs. S8H–J in Supporting information).

The enterobacterial composition of all testing mice was analyzed by 16S rRNA gene sequencing. A flower plot (Fig. 4A) was generated to display the number of common and endemic species at the genus level, visualizing the overlap among samples. The results showed that the gut microbiota of healthy mice was dominated by *Bacillota* and *Bacteroidota*, while harmful *Pseudomonadota* only accounted for 3.8% of the microbiota. DSS treatment significantly reduced both the total microbial load and diversity, as indicated by decreased Chao and Shannon index values in the model group compared to the normal control (Figs. 4B and C). Principal components analysis (PCA) and non-metric multidimensional scaling (NMDS) analyses indicated a tendency for microbiota aggregation, showing a clear distinction between the DSS-treated mice and the healthy mice (Figs. 4D and E). Additionally, DSS treatment notably altered the balance between harmful and beneficial bacteria, with the proportion of endotoxin-producing *Pseudomonadota* increasing to 79.5% (Fig. 4F). Treatment of free PAO increased the abundance and diversity of the gut microbiota, increased Chao and Shannon index values, and minimized the distribution distances with the healthy control. Notably, a decrease in the relative abundance of *Enterobacteriaceae* along with the increased relative abundance of *Lachnospiraceae*, *Muribaculaceae*, and *Bacteroidaceae* was observed after PAO treatment (Figs. 4G–J). Due to the site-specific release of PAO from the pellets that enabled higher drug concentrations in the colon, PAO-βCD@pellet demonstrated the most prominent effect in restoring the gut microbiota. This might represent an additional mechanism by which PAO alleviates DSS-induced IBD.

PAO exhibits broad pharmacological activities. PAO and its active components (PA, PO, and PE) exert therapeutic effects on a number of inflammatory intestinal targets *via* multiple pathways. For example, PE protects against DSS-induced barrier disruption *via* Rho-associated kinase 1/myosin light chain 2 (ROCK1/MLC2) pathway [28] and exerts anti-inflammatory effects through the Toll like receptors 4/myeloid differentiation primary response 88/nuclear factor kappa-B (TLR4/MyD88/NF-κB) pathway [28]. Whereas PA alleviates 5-fluorouracil-induced intestinal mucositis by modulating the intestinal flora and regulating the TLR2/MyD88/NF-κB pathway [29]. Meanwhile, PA promotes macrophage repolarization from

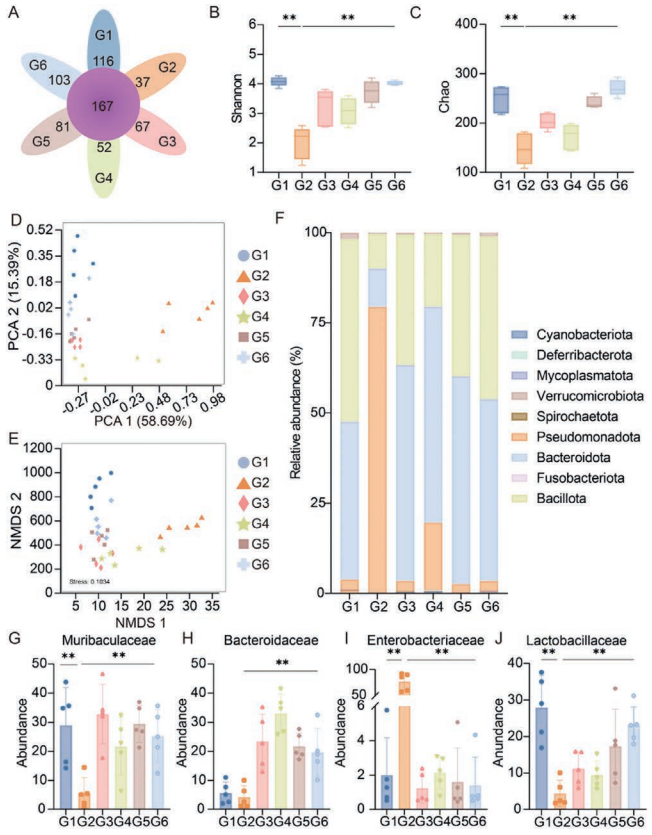


Fig. 4. Gut flora analysis of mice after different treatment. (A) Flower plot of identified bacterial strains. (B) Chao indexes. (C) Shannon indexes. (D) PCA score plots of flora species. (E) NMDS score plots of flora species. (F) The relative abundance of gut microbiomes at the phylum level. (G–J) are *Muribaculaceae*, *Bacteroidaceae*, *Enterobacteriaceae*, and *Lachnospiraceae*, respectively. Data are presented as means ± SD ($n = 5$). $^{**}P < 0.01$.

inflammatory M1 type *via* the threonine kinase (Akt)/mitogen-activated protein kinase (MAPK)/NF-κB pathway [30]. Diarrhea is another typical symptom of IBD caused by impaired intestinal water absorption, which can be mitigated by PA *via* the vasoactive intestinal peptide-cyclic adenosine monophosphate-protein kinase A (VIP-cAMP-PKA) pathway [31]. Additionally, PAO inhibits ROS-induced pyroptosis and reduces inflammation-induced damage to epithelial cells [15]. However, the therapeutic activity of PA is dose-dependent, with effective concentrations generally ranging from 10 μmol/L to 40 μmol/L *in vitro* [32]. To increase the concentration of PAO at inflammatory sites, previous studies utilized intravenous injection, leveraging the EPR effect (Enhanced permeability and retention effect) of inflamed tissues [33]. Liposomes modified with lactoferrin were used as carriers to enhance drug accumulation at inflammation sites, thus improving IBD treatment outcomes [34]. Compared to intravenous injection, oral administration offers better patient compliance and allows the drug to directly reach the inflamed colon [2]. However, PAO's instability in gastric acid reduces its effective dose, and oral absorption followed by first-pass metabolism in the liver further decreases the drug's concentration in the inflammatory colon [2]. Therefore, the development of a colon-targeted drug delivery system is crucial for improving PAO concentrations in the colon and ensuring effective IBD treatment.

Mesoporous silica adsorption and cyclodextrin inclusion are common pharmaceutical strategies for stabilizing volatile oils [35]. Silica adsorption utilizes hydrogen bonding, mesoporosity, and hydrophobic interactions to encapsulate the drug, enhancing the dispersion of poorly soluble drugs in water and providing sustained release [15]. However, physical adsorption does not significantly improve the stability of volatile oils, and the presence of both surface and mesopore adsorption may lead to incomplete drug release [36]. Cyclodextrin inclusion, on the other hand, utilizes the hydrophobic cavity of cyclodextrin to encapsulate poorly soluble drugs, significantly improving stability and solubility while protecting against environmental factors like high temperature and ultraviolet (UV) exposure [37]. However, inclusion complexes are generally amorphous and require excessive cyclodextrin to achieve effective encapsulation, which increases the cost [38]. In comparison, inclusion cocrystals offer a distinct advantage, combining the benefits of both cocrystals and inclusion complexes [19]. As cocrystals, PAO and cyclodextrin form an ordered structure with a fixed stoichiometric ratio, exhibiting defined melting points, crystal structures, and higher stability. At the same time, inclusion cocrystals rapidly release the PA-cyclodextrin complex, offering good solubility and stability under acidic, alkaline, and UV conditions [39]. Importantly, inclusion cocrystals are patentable solid forms, which is crucial in new drug development.

While PAO-βCD cocrystals significantly improve PAO stability and solubility, their rapid dissolution upon oral administration results in fast drug release in the stomach, reducing the concentration of PAO at the inflamed colon site. To address this, we prepared PAO-βCD cocrystals into pellets, which were then coated by a pH-sensitive material (*e.g.*, Eudragit®) to form PAO-βCD@pellet. The results demonstrated that the PAO-βCD@pellet exhibited remarkable pH responsiveness, releasing PAO rapidly at the colonic site, thus enhancing drug exposure at the site of inflammation. Consequently, the treatment effectively suppressed inflammation, strengthened colonic barrier function, restored water absorption, and contributed to immune modulation and gut microbiota remodeling, collectively supporting its therapeutic potential.

In conclusion, the development of PAO-βCD@pellet represents a significant advancement in the oral delivery of PAO for the treatment of IBD. By leveraging the merits of βCD inclusion cocrystals and pH-sensitive coating, this formulation ensures the targeted release of PAO at the inflamed colon, thereby overcoming challenges related to the drug's instability in the acidic stomach and minimizing off-target intestinal adsorption. Our results from both *in vitro* and *in vivo* studies demonstrated the enhanced therapeutic efficacy of PAO-βCD@pellet, evidenced by improved disease outcomes, reduced intestinal inflammation, and protection of the intestinal barrier in the DSS-induced colitis model. Additionally, the formulation showed promising benefits in modulating the gut microbiome, suggesting a dual mechanism of action in IBD treatment. This study highlights the potential of PAO-βCD@pellet as a novel and effective treatment option for IBD, providing a promising approach for the clinical application of traditional herbal medicines in gastrointestinal disorders.

Declaration of competing interest

The authors declare that they have no known competing financial interests or personal relationships that could have appeared to influence the work reported in this paper.

CRediT authorship contribution statement

Zeyu Li: Writing – original draft, Validation, Investigation, Formal analysis, Data curation. **Huan Shen:** Validation, Methodology, Formal analysis, Conceptualization. **Wenli Cai:** Visualization, Validation, Formal analysis, Data curation. **Quangang Xu:** Visualization, Validation, Formal analysis. **Wei Xia:** Visualization, Methodology, Data curation. **Keke Ning:** Methodology, Formal analysis, Data curation. **Ergang Liu:** Project administration, Investigation, Conceptualization. **Yongzhuo Huang:** Writing – review & editing, Super-

vision, Resources, Project administration, Methodology, Funding acquisition, Conceptualization.

Acknowledgments

We are thankful for the support from the National Key Research and Development Program of China (Nos. 2022YFE0203060, 2024YFA1210204), National Natural Science Foundation of China (Nos. 82341232, 82404549), the Future Network (No. 083GJHZ2023012FN) and Grand Challenges (No. 083GJHZ2023021GC) of the International Partnership Program of the Chinese Academy of Sciences, CAS President's International Fellowship Initiative (No. 2024VBB0004), the High-level Innovative Research Institute from Department of Science and Technology of Guangdong Province (No. 2021B0909050003), and Zhongshan Municipal Bureau of Science and Technology (Nos. LJ2021001, CXTD2022011), the Second Batch of Social Welfare and Basic Research Projects of Zhongshan City (No. 2023B2033). This work was also supported by Natural Science Foundation of Shanghai Municipal (No. 24ZR1477500). We acknowledge the use of Grammarly and Deepseek to help review the writing of the manuscript to improve the readability and language of the work. The authors reviewed and edited the content at the final stage and took full responsibility for the content of the publication.

Supplementary materials

Supplementary material associated with this article can be found, in the online version, at doi:10.1016/j.cclet.2025.111292.

References

[1] A. Sudabeh, G.S. Sadaf, I. Kevin, et al., Lancet Gastroenterol. Hepatol. 5 (2020) 17–30.
[2] S. Jing, H. Chen, E. Liu, et al., Carbohydr. Polym. 316 (2023) 121025.
[3] M.J. Friedrich, JAMA 319 (2018) 648.
[4] F. Wang, H. Yao, X. Wu, et al., Chin. Chem. Lett. 35 (2024) 108821.
[5] S. Singh, J.R. Allegretti, S.M. Siddique, J.P. Terdiman, Gastroenterology 158 (2020) 1465–1496.
[6] S. Honap, V. Jairath, S. Danese, L. Peyrin-Biroulet, Nat. Rev. Drug Discovery 23 (2024) 546–562.
[7] K. Bechman, M. Yates, J.B. Galloway, Pharmacol. Res. 147 (2019) 104392.
[8] M. Sun, W. Ban, H. Ling, et al., Chin. Chem. Lett. 33 (2022) 4449–4460.
[9] J. Yang, K. Wang, S. Sun, et al., Chin. Chem. Lett. 36 (2025) 110180.
[10] S. Singh, J. George, B.S. Boland, N. Vande Casteele, W.J. Sandborn, J. Crohns Colitis 12 (2018) 635–643.
[11] L. Yin, X. Jiang, M. Wang, et al., Chin. Chem. Lett. 36 (2025) 110224.
[12] J. Wang, Y. Chen, L. Han, et al., Chin. Chem. Lett. 35 (2024) 109029.
[13] J. Zhang, A. Ou, X. Tang, et al., J. Nanobiotechnology 20 (2022) 389.
[14] P.L.B. Jain, S.R. Patel, M.A. Desai, J. Essent. Oil Res. 34 (2022) 1–11.
[15] H. Chen, L. Pan, C. Zhang, et al., Adv. Healthcare Mater. 13 (2024) 2400566.
[16] Y. Huang, P. Zhao, X. Zhang, H. Fu, C. Fu, J. Ethnopharmacol. 336 (2025) 118737.
[17] R. Guo, W. Xu, Y. Wang, et al., ACS Appl. Mater. Interfaces 16 (2024) 29198–29209.
[18] L.E. McCoubrey, A. Favaron, A. Awad, et al., J. Control. Release 353 (2023) 1107–1126.
[19] H. Shen, L. Pan, K. Ning, et al., J. Nanobiotechnology 22 (2024) 119.
[20] G.A. Vega, J.A. Dávila, Nat. Prod. Res. 36 (2022) 4193–4199.
[21] S. Wang, Z. Liu, Y. Tong, et al., J. Control. Release 330 (2021) 483–492.
[22] X. Yan, Z. Huang, Y. Wu, et al., Int. J. Pharm. 610 (2021) 121234.
[23] X. Song, Q. Huang, Y. Yang, et al., Adv. Mater. 35 (2023) 2301585.
[24] C. Danne, J. Skerniskyte, B. Marteyn, H. Sokol, Nat. Rev. Gastroenterol. Hepatol. 21 (2024) 184–197.
[25] J. Zhang, Y. Zhao, T. Hou, et al., J. Control. Release 320 (2020) 363–380.
[26] A. Bhattacharyya, R. Chattopadhyay, S. Mitra, S.E. Crowe, Crowe, Physiol. Rev. 94 (2014) 329–354.
[27] L.A. Kiyuna, R.P. Albuquerque, C.H. Chen, D. Mochly-Rosen, J.C.B. Ferreira, Free Radical Biol. Med. 129 (2018) 155–168.
[28] Y. Liu, J. Wu, L. Chen, et al., Biochem. Pharmacol. 182 (2020) 114260.
[29] J. Wu, Y. Gan, M. Li, et al., Biomed. Pharmacother. 124 (2020) 109883.
[30] Y. Wu, S. Wan, S. Yang, et al., J. Nanobiotechnology 20 (2022) 542.
[31] Y. Gan, G. Ai, J. Wu, et al., J. Ethnopharmacol. 250 (2020) 112519.
[32] Y.F. Xian, Y.C. Li, S.P. Ip, et al., Exp. Ther. Med. 2 (2011) 545–550.
[33] P.V.L. Santos, L.B. Jerônimo, W.S.C. Ribeiro, et al., Front. Pharmacol. 15 (2024) 1966–1976.
[34] Y. Zhao, Y. Yang, J. Zhang, et al., Acta Pharm. Sin. B 10 (2020) 1966–1976.
[35] L. Stjern, S. Voittonen, R. Weldemichel, et al., Int. J. Pharm. 531 (2017) 595–605.
[36] S.S. Hate, S.M. Reutzel-Edens, L.S. Taylor, Mol. Pharmaceut. 17 (2020) 3435–3446.
[37] A. Aman, S. Ali, L. Oopkaew, et al., J. Mol. Liq. 411 (2024) 125645.
[38] S. Yi, T. Guo, Y. Wang, et al., Carbohydr. Polym. 350 (2025) 123042.
[39] W. Gu, Y. Liu, J. Mol. Struct. 1201 (2020) 127159.